A study of the diameter influence on the fluid force of two tandem cylinders

*Zhenhua Song[1], Menglan Duan[2] and Jijun Gu[3]

[1), 2), 3)] *Offshore Oil/Gas Research Center, China University of Petroleum, Beijing, 102249, China*
[1)] *thzh83@163.com*

ABSTRACT

The diameter ratio influence of laminar flow past two tandem cylinders at Reynolds number of 1400 is numerically investigated in this study. The effects of two cylinder diameter ratio d/D on the hydrodynamics of tandem cylinders are evaluated. Three distinct flow regimes are identified based on the mechanism of lift and drag force variation. The amplitude of lift coefficient and drag coefficient on both large cylinder and small cylinder increases in Regime 1, decrease in Regime 2, and increased again in Regime 3. In Regime 2, the amplitude of drag coefficient nearly converges to zero and the lift force on both cylinders decreases rapidly, meanwhile, in all of the three regimes, the drag force on large cylinder decreases, whereas, the drag force on small cylinder increase. From d/D=0.875 to d/D=1,the drag force is opposite to streamwise.

1. INTRODUCTION

Multiple circular cylinders placed one behind the other in flow are widely application in many ocean engineering, such as spr platform, risers, subsea pipeline and many offshore structures. Normally, the situation of two cylinders can be placed as tandem, side-by-side and staggered arrangements. These situations have been the subject of a lot of numerical and experimental studies by different researchers. In this respect, fluid forces interaction between two circular cylinders in tandem and side-by-side arrangements was studied experimentally by some researchers. The interactions of two adjacent bodies may change the hydrodynamic of an individual object. A well-known example is the flow over two cylinders in tandem arrangement (Zdravkovich, 1977; Slaouti and Stansby, 1992). Compared with an isolated cylinder, the drag coefficient of the downstream cylinder can be reduced, which is attributed to the suppression of vortex shedding from the upstream cylinder. The flow past two fixed circular cylinders at Reynolds numbers of 102 and 103, using the finite-element method (FEM) performed 2-D numerical simulations. (Mittal, S., Kumar, V., Raghuvanshi, A., 1997). The Researchers found that vortices were not formed from the upstream cylinder at Re=102, but were observed at Re=103, at gaping ratio L/D=2.5. Through the experiments, they found that vortex shedding of upstream cylinder is suppressed with L/D<3. In the research, a constant flow past two tandem cylinder and side-by-side arrangements at

---

[1)] Ph.D. Candidate
[2)] Professor
[3)] Professor

Re=102 and 2×102 using a 2-D FEM, the researchers found the critical spacing ratio is very sensitive to the Reynolds number.(Meneghini, et al, 2001). Another important research in 2003, though the simulation of tandem cylinders at Re=80 and 103 with 2D-FEM. The drag coefficient of upstream and downstream cylinders performed different values from L/D gradually increase from1.9 to 2.5 method and L/D decreased from 2.5 to1.9 method. Laneville and Brika (1999) investigated the effect of mechanical of two same diameter cylinders.   In their research, the upstream cylinder is little influenced by tandem arrangement configuration, liking an isolate cylinder behaviors in the same flow condition, whereas, the response of downstream cylinder is sensitive with the spacing ratio of the tandem cylinders. The responses of both the cylinders were found to be hysteretic in nature.In addition, many researchers have been carried out by Bearman and Wadcock, Liu et al., Roy et al., they applied a flow visualization method to study the interaction of two side-by-side circular cylinders at Re = 2.5×104 .

Nomenclature	
f_s	Vortex shedding frequency
R_e	Reynolds number($R_e = \frac{UD}{\upsilon}$)
d	Diameter of small cylinder
D	Diameter of large cylinder
F_x	Dimensional drag force exerted on unit length of the circular cylinder
F_y	Dimensional lift force exerted on unit length of the circular cylinder
C_L	Lift coefficient
C_D	Drag coefficient
C_L^{RMS}	Root mean square value of lift coefficient
C_D^{MEAN}	Time-average mean drag coefficient
C_L^{MAX}	The maximum value of lift coefficient
C_D^{MAX}	The maximum value of drag coefficient
C_L^{MIN}	The minimum value of lift coefficient
C_D^{MIN}	The minimum value of drag coefficient
$d\_C_D^{MAX}$	The maximum value of drag coefficient of bare circular cylinder
$(D)d\_C_D^{MAX}$	The maximum value of drag coefficient of front circular cylinder in tandem cylinders
$(d)D\_C_D^{MAX}$	The maximum value of drag coefficient of back circular cylinder in tandem cylinders
U	Free-stream velocity
μ	Dynamic viscosity of the fluid
υ	Kinematic viscosity of the fluid
ω	vortices

As described above, numerical investigations on flows past two circular cylinders with different arrangement have been performed recently. Most of these numerical studies, however, employed a 2-D analysis and investigated the flow characteristics on variation of spacing ratio of two cylinders.

In this work, we study the fluid forces of an arrangement of two circular cylinders by numerical simulation. Two tandem cylinders are placed in uniform flow, the fluid force is investigated under various diameter ratio. We found the fluid force on upstream cylinder is sensitive with 0.25<d/D<0.5, whereas, the sensitive range of downstream cylinder is 0.375<d/D<0.625. Comparing with results of previous numerical studies, the characteristics of the flow pattern and the fluid-induced forces obtained from the computations are investigated.

2. NUMERICAL MODEL

2.1 GOVERNING EQUATIONS

The two dimensional Navier-Stokes equations for the incompressible fluids are expressed as follow:

$$\frac{\partial u}{\partial x} + \frac{\partial v}{\partial y} = 0 \tag{1}$$

$$\frac{\partial u}{\partial t} + u\frac{\partial u}{\partial x} + v\frac{\partial u}{\partial y} = -\frac{1}{\rho}\frac{\partial p}{\partial x} + v\left(\frac{\partial^2 u}{\partial x^2} + \frac{\partial^2 u}{\partial y^2}\right) \tag{2}$$

$$\frac{\partial v}{\partial t} + u\frac{\partial v}{\partial x} + v\frac{\partial v}{\partial y} = -\frac{1}{\rho}\frac{\partial p}{\partial y} + v\left(\frac{\partial^2 v}{\partial x^2} + \frac{\partial^2 v}{\partial y^2}\right) \tag{3}$$

The drag coefficient and lift coefficient on the cylinder are described by following equation:

$$C_L(t) = \frac{F_y(t)}{0.5\rho U^2 DL} \tag{4}$$

$$C_D(t) = \frac{F_x(t)}{0.5\rho U^2 DL} \tag{5}$$

The time averaged mean drag coefficient C_D^{MEAN} is described as:

$$C_D^{MEAN} = \int_{t1}^{t2} C_D(t)dt/\Delta T \tag{6}$$

The Root mean square (RMS) of lift coefficient is described as:

$$C_L^{RMS} = \left(\int_{t1}^{t2} \left(C_L(t) - C_L^{MEAN} \right)^2 dt / \Delta T \right)^{\frac{1}{2}} \tag{7}$$

$$f_s = St \frac{U}{D} \tag{8}$$

Where the vortex shedding frequency f_s is the same as the frequency of the lift fluctuation, and is obtained by Fast Fourier Transform (FFT) analysis of the lift coefficient.

2.2 computational domain and boundary conditions

In the present study, two tandem cylinders of different diameters are arranged in a 40D×20D rectangular domain. The center of downstream cylinder is located at 10D back of the inlet boundary. The distance between two cylinder surfaces is 0.5D, and the distance from downstream cylinder center to outlet is 30D. There are both 10D distance of the upper and lower boundaries from the center of the two cylinders. Where the D is diameter of the downstream cylinder, d is diameter of the upstream cylinder. The cylinders boundaries are no slip boundaries. There are various d/D ranging from 0.125 to 1 with increment of 0.125. Fig.1 shows the geometry of domain and relative location of cylinders. l means the gap spacing between two cylinder wall surfaces.
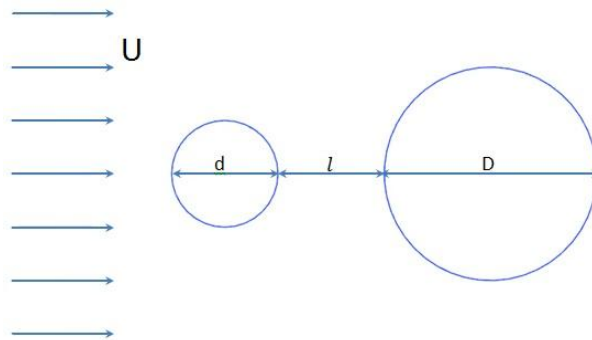

Fig.1 Schematic of location of cylinders in tandem arrangement

The boundary conditions are summarized as follows. At the inlet boundary, a uniform velocity profile is imposed. And the traction free condition ($\partial u/\partial x = \partial v/\partial x = 0$) is given at outlet, the symmetric conditions ($\partial u/\partial y = 0, v = 0$) are imposed on the other sides of the boundaries.

Table1 Results of flow around a fixed cylinder, Re=185

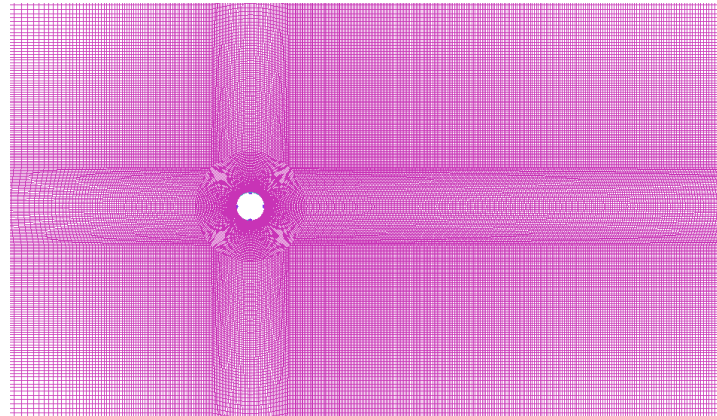|	C_L^{RMS}	C_D^{MEAN}	St
This article	0.433	1.308	0.198
Lu and Dalton	0.422	1.310	0.195
Guilmineau	0.443	1.287	0.195

Fig. 2 typical computational meshes near two cylinders

3. FLOW PAST TWO CIRCULAR CYLINDER IN TANDEM ARRANGEMENT

The variations of d/D may influence the flow past two tandem circular cylinders of different diameters. The influence from this factor with identification of flow regimes will be examined with various detailed analysis in this section.

3.1 INFLUENCE OF VARIOUS D/D ON FLUID FORCE COEFFICIENT OF TWO TANDEM CIRCULAR CYLINDERS

In the section, the fluid force coefficients are contrasted though 9 Figures and 4 Tables. Three distinct Regimes can be clearly identified in the figures. In Regime 1 of 0.125<d/D<0.375,the C_L^{RMS} on large cylinder is relatively stable and the lift force coefficient of small cylinder has a little increasing. In Regimes 2, the C_L^{RMS} on both cylinders are decreases rapidly with the increase in d/D, especially in 0.375<d/D<0.5, the C_L^{RMS} is observed to decrease abruptly with the increase in d/D, in this Regime, the C_D^{MAX} and C_D^{MIN} seem to converge to one point, which is a narrow band covering 0.5<d/D<0.875, the C_D^{MAX} -C_D^{MIN} on small cylinder is observed to close to zero In Regime 3, the C_L^{RMS} on large cylinder continues decreasing with the d/D, but C_L^{RMS} on small cylinder becomes increasing again.

Table 2 Comparison of C_L^{MAX} 、 C_L^{MIN} 、 C_L^A

| d/D	d_C_L^{MAX}	(D)d_C_L^{MAX}	(d)D_C_L^{MAX}	d_C_L^{MIN}	(D)d_C_L^{MIN}	(d)D_C_L^{MIN}	d_C_L^A	(D)d_C_L^A	(d)D_C_L^A
0.125	0.451	0.485	1.854	-0.450	-0.485	-1.836	0.901	0.97	3.659
0.25	0.656	0.822	1.993	-0.657	-0.812	-1.984	1.313	1.634	3.977
0.375	1.106	1.022	2.037	-1.106	-0.950	-2.097	2.212	1.972	4.134
0.5	1.215	0.305	1.099	-1.214	-0.304	-1.106	2.429	0.609	2.205
0.625	1.334	0.207	0.791	-1.334	-0.206	-0.792	2.668	0.413	1.583
0.75	1.480	0.199	0.723	-1.498	-0.197	-0.722	2.978	0.396	1.445
0.875	1.515	0.195	0.622	-1.511	-0.199	-0.617	3.026	0.394	1.239
1	1.820	0.406	0.753	-1.821	-0.423	-0.775	3.641	0.829	1.528
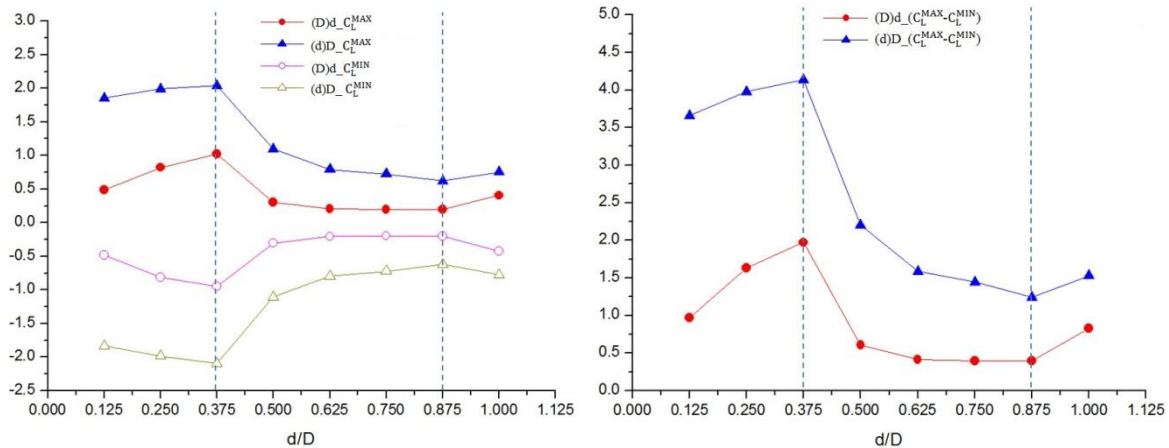
Fig.3 Variation of C_L^{MAX}, C_L^{MIN} for different diameter ratio d/D
Fig.4 Variation of C_L^A for different diameter ratio d/D

In the whole region, 0.125<d/D<1, the maximum of lift coefficient line is symmetric with the minimum of lift coefficient line, and C_L^A have particular characteristics in each Regime.

In Regime 1 of 0.125<d/D<0.375, the maximum value of lift coefficient on both cylinders increase and the minimum value of drag coefficient on both cylinders decrease with the increase in d/D. The maximum line and minimum line separates with each other with the increase in G/D. In Regime 2, the maximum of lift coefficient line and the minimum of lift coefficient line become approaching each other, these two lines become separate with each other again in Regime 3. So the ups and downs of the value of C_D^A is clearly identified in Fig.4. The C_L^A line of large cylinder is parallel with C_L^A line of small cylinder.

Table3 Comparison of C_D^{MAX} 、 C_D^{MIN} 、 C_D^A

d/D	d_C_D^{MAX}	(D)d_C_D^{MAX}	(d)D_C_D^{MAX}	d_C_D^{MIN}	(D)d_C_D^{MIN}	(d)D_C_D^{MIN}	d_C_D^A	(D)d_C_D^A	(d)D_C_D^A
0.125	0.947	0.667	1.833	0.895	0.496	0.951	0.052	0.171	0.882
0.25	0.951	0.771	1.783	0.843	0.425	0.710	0.108	0.346	1.073
0.375	1.203	0.971	1.921	0.957	0.450	0.395	0.246	0.521	1.526
0.5	1.480	0.695	0.967	1.120	0.661	0.501	0.360	0.034	0.466
0.625	1.570	0.785	0.506	1.140	0.782	0.290	0.430	0.003	0.216
0.75	1.729	0.839	0.267	1.185	0.834	0.075	0.544	0.005	0.192
0.875	1.734	0.906	-0.018	1.156	0.901	-0.157	0.578	0.005	0.139
1	1.979	0.995	0.109	1.1625	0.920	-0.452	0.816	0.075	0.561
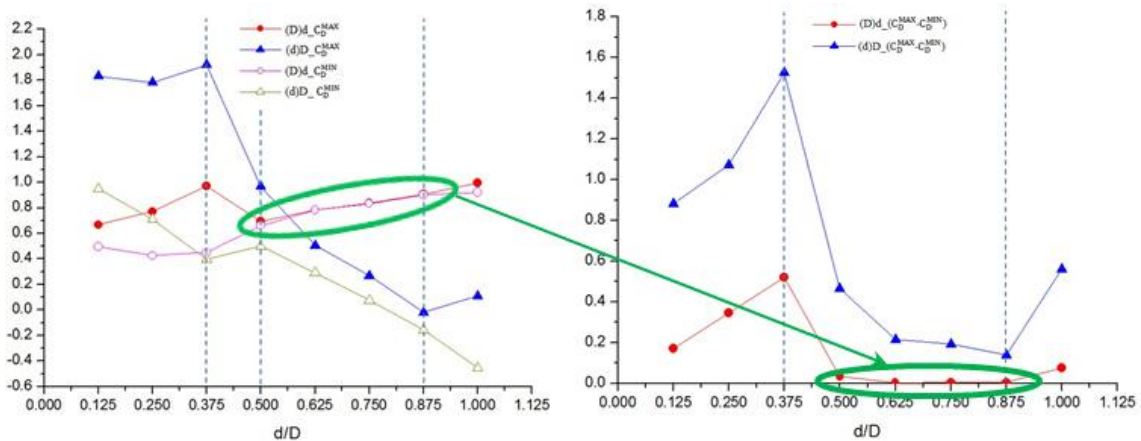
Fig5. Variation of C_D^{MAX}, C_D^{MIN} for different diameter ratio d/D
Fig6. Variation of C_D^A for different diameter ratio d/D

The tendency of C_D^{MAX}, C_D^{MIN} and C_D^A on both cylinders is very similar to C_L^{MAX} 、 C_L^{MIN} 、 C_L^A on both cylinder, The C_D^A line of large cylinder is also parallel with C_D^A line of small cylinder. The special characteristic of C_D is the small cylinder in Regime 2, 0.5<d/D<0.875,the C_D^{MAX} is very close to C_D^{MIN} of small cylinder and seem to converge to one point, this phenomenon is reflect in Fig.5 that C_D^A of small cylinder is very close to zero. It implies extremely weak drag fluctuation on small cylinder. The phenomenon of drag coefficient is induced by the change in flow pattern which will be examined later on. As the diameter ratio d/D>0.5, both C_L^A and C_D^A is found to have little dependence on the diameter ratio d/D.

In Regime 1, 0.125<d/D<0.375, the lift coefficient of large cylinder keeps in a relatively steady value compared with the lift coefficient of small cylinder jumps to a high value at d/D=0.375. As the fluctuation of the C_L increases in 0.25<d/D<0.375, the value of C_L^{RMS} on small cylinder abuptly increase. Comparded with small cylinder, the

value of C_L^{RMS} large cylinder is more flat than small one, that means the influence of diameter ratio d/D on the C_L^{RMS} is very weak.

Table4 Comparison of C_L^{RMS} and C_D^{MEAN}

d/D	d_C_L^{RMS}	(D)d_C_L^{RMS}	(d)D_C_L^{RMS}	d_C_D^{MEAN}	(D)d_C_D^{MEAN}	(d)D_C_D^{MEAN}
0.125	0.318	0.317	1.153	0.921	0.571	1.437
0.25	0.464	0.311	1.176	0.898	0.541	1.299
0.375	0.758	0.497	1.165	1.084	0.688	1.117
0.5	0.863	0.206	0.776	1.308	0.678	0.739
0.625	0.956	0.144	0.551	1.371	0.784	0.401
0.75	1.057	0.137	0.503	1.480	0.837	0.173
0.875	1.081	0.136	0.430	1.471	0.903	-0.089
1	1.196	0.187	0.366	1.596	0.952	-0.283
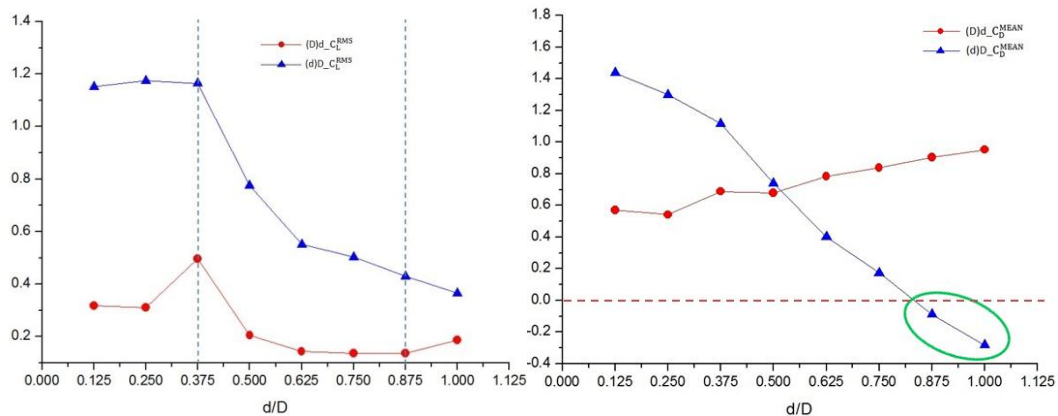
Fig.7 Variation of C_L^{RMS} for different diameter ratio d/D
Fig.8 Variation of C_D^{MEAN} for different diameter ratio d/D

In Regime 2, both of the C_L^{RMS} values on tandem cylinders become decrease rapidly, the value of large cylinder keep descrease in the whole Regime 2, while the value of C_L^{RMS} on small cyliner keeps in a steady value in 0.625<d/D<0.875, it implies the C_L^{RMS} is not sensitive to the diameter ratio d/D in this range.

In Regime 3, the C_L^{RMS} on large cylinder continues decreasing with the increasing d/D, but the C_L^{RMS} on small one become increase in this Regime. Thus, the phenomenon account for the C_L^{RMS} is not always keeping decrease with the increase in d/D

It denotes a strong linear relationship between C_D^{MEAN} and d/D on both cylinders. The small one increases with d/D, and the large one is opposite, especially 0.875<d/D<1, the C_D^{MEAN} on large cylinder becomes an negtive value, means the direction of C_D^{MEAN} is opposite to streamwise.
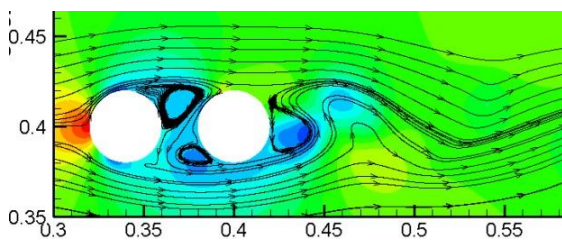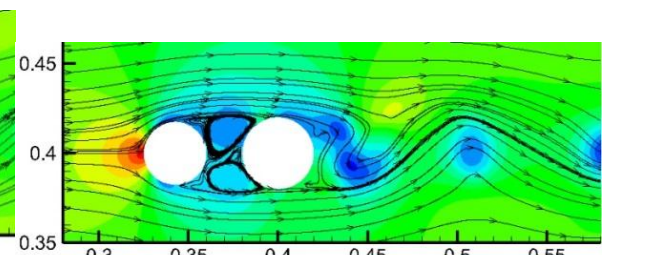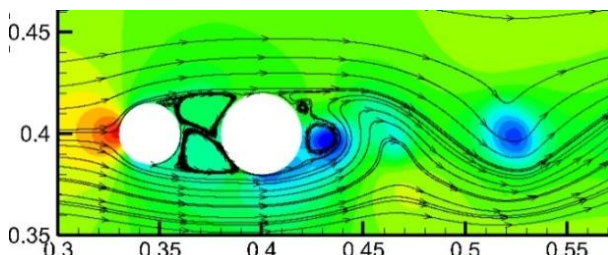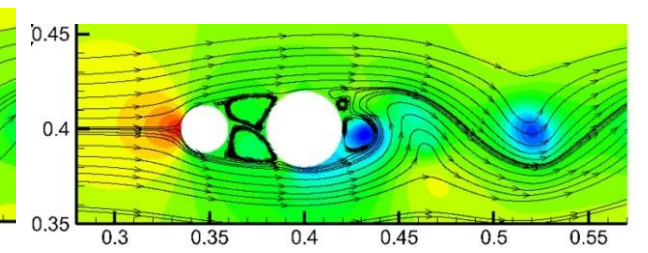
Fig.9 (a) bare cylinder

Fig.9 (b)   d/D=0.125

Fig.9(c) d/D=0.25

Fig.9 (d) d/D=0.375

Fig.9 (e)   d/D=0.5

Fig.9 (f) d/D=0.625

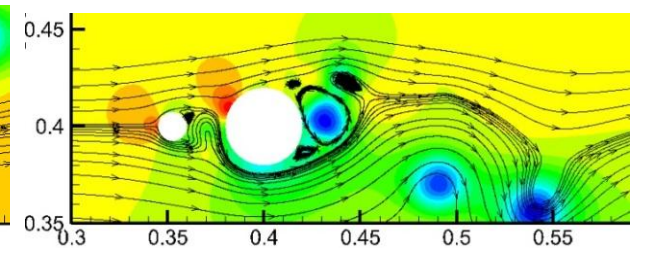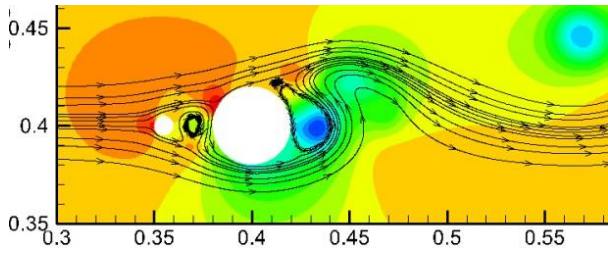Fig.9(g) d/D=0.75
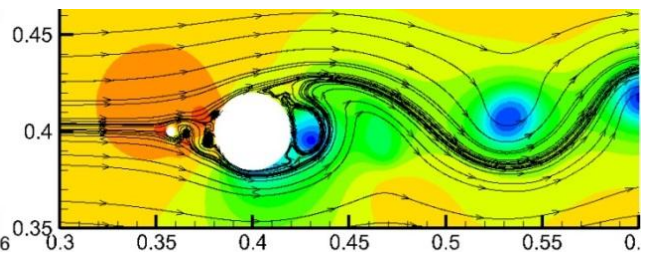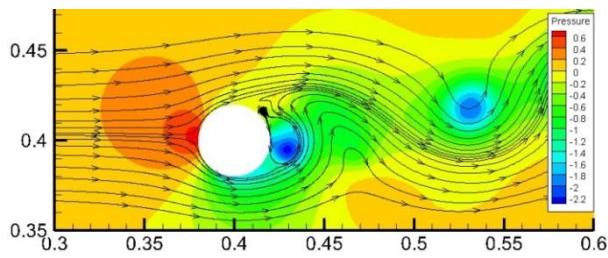
Fig.9 (h)   d/D=0.875
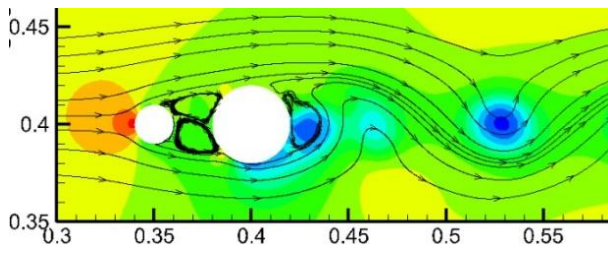
Fig.9(i) d/D=1

3. 2 MECHANISMS OF FLUID FORCE REDUCTION ON TANDEM CYLINDERS

The numerical results have shown that the fluid forces on the large cylinder can be reduced significantly in tandem arrangement at low Reynolds number. The mechanisms associated with the fluid force reduction are inspected as follow.

Fig.9 shows the contours of the pressure field and the streamlines around the tandem cylinders. Eight different diameter ratios d/D are examined. Each Figure on the pressure filed corresponds to the point of the largest negative lift coefficient. For the comparison on the reduction of fluid force, the flow pattern and pressure field of the bare cylinder of D diameter is also included.

(1)Regime2：0.125<d/D<0.375

It can be seen that the flow pattern of the tandem cylinders in Fig9.(b) and Fig9.(c) is very similar to that observed for bare cylinder in Fig.9(a). Under a very large diameter ratio d/D, the tandem cylinder behaves as a bare one. However, due to the existence of small cylinder, the vortex shedding frequency ($f_s = 1.414$) of small cylinder is far higher than the frequency ($f_s = 0.227$) of large cylinder, results the high pressure of large cylinder moves to the right of top side, the offset of the pressure lead to the lift force component of fluid force increase, and the drag force component of fluid force decrease. However, the lift force of the large increases very little, as there are two small vortexes shedding by small cylinder reach to the front of the large cylinder, the small vortex counteract part influence of lift force induced by the offset of high pressure. Fig.9(d) is the limiting case of the Regime 1, corresponding to the large offset of high pressure, the top side pressure of the large cylinder is reduced much more than previous.

On the account of Regime 1, it can be seen in Table 2 that D_C_L^A=3.641 on bare cylinder D and d/D=0.125,0.25,0.375, (d)D_C_L^A=0.659,0.3977,1.134, the variation ratio is smaller than 0.1, d_C_L^{RMS} =1.196 on bare cylinder D and d/D=0.125,0.25,0.375, d(D)_ C_L^{RMS} =1.153, 1.176, 1.165, the variation ratio is smaller than 0.01, thus, the tandem arrangement has limited influence on the C_L^A and C_L^{RMS}. It can be seen that the variation of the drag coefficient much larger than the lift coefficient on large cylinder. D_C_D^A=0.816 on bare cylinder, and d/D=0.125,0.25,0.375, (d)D_C_D^A=0.081,0.315,0.87, consequently, the influence on drag coefficient is much larger than the drag coefficient in Regime 1.

(2)Regime2：0.375<d/D<0.875

Fig.9(f) is a typical flow pattern in Regime2. It can be seen clearly that the high pressure in upstream of large cylinder has disappeared. Instead of the high pressure, the symmetric vortexes structure with respect to the center line between small cylinder and large cylinder are well retained. Meanwhile, the pressure difference between the upstream and downstream sides of the large cylinder is reduced, leading to a reduction in the mean drag force on the large cylinder. Similarly, the lift force is reduction by smaller pressure difference.

It appears that the flow transitions from Regime1 to Regim2 from Fig.9(e). From this Figure, two small moderate high pressure areas have been found in front of the large cylinder wall, these two small moderate high pressure areas are symmetric areas with respect to the center line, thus these have little influence on lift force.

From Table 2 and Fig.3, the values of C_L^{MAX} and C_L^{MIN} are getting close to each

other, C_L^A become lower and lower in Regime 2, It implies two cylinders have strong interaction with each other, leading to the fluid forces suppressed by the interaction. The effect of the suppression increases with the increases in d/D. during 0.375<d/D<0.5, (D)d_C_D^{MAX} 、 (d)D_C_D^{MAX} become decreases and (D)d_C_D^{MIN} , (d)D_ C_D^{MIN} increases rapidly, leading to the value of (D)d_C_D^A、 (d)D_C_D^A at d/D=0.5 rather large than the value of (D)d_C_D^A、(d)D_C_D^A at d/D=0.375, especially the value of (D)d_C_D^{MAX} and (D)d_C_D^{MIN} is nearly converge to the same value of (D)d_ C_D^{MAX} =0.695 and (d)D_ C_D^{MIN} =0.661, (D)d_C_D^A=0.034. It means nearly no drag fluctuation on small cylinder at this point. This state keeps a long rang form d/D=0.5 to d/D=0.875 in Regime 2. Although the drag fluctuation decreases, (D)d_C_D^{MEAN} increase gradually, and (d)D_C_D^{MEAN} also decrease in Regime 2.

In Fig.9(h), it can be seen the pressure around the large cylinder is very different from Fig.9(g), the downstream pressure of the large cylinder is large than the upstream pressure that the C_D^{MEAN} becomes to an negative value, it means the drag force opposite to the streamwise at d/D=0.875.

(3)Regime3：0.875<d/D<1

It needs to pay special attention to the transition of flow pattern at d/D=1. The equal and symmetric vortexes structure between tandem cylinders is broken. The down side vortex size becomes smaller than upside vortex size, leading to smaller largest negative lift force corresponding to Fig. 2. Meanwhile the upstream pressure of the large cylinder is lower than the same instant at d/D=0.875, results to the continuous decrease of C_D^{MEAN} .

4. CONCLUSION

The numerical results of fluid flow past two tandem cylinders at low Reynolds number are presented in this work. The effect of diameter ratio d/D on fluid forces and flow patterns are investigated. Three flow Regimes are distinguished according to variation of fluid force.

In Regime 1, when the d/D increases, the amplitude of lift coefficient and drag coefficient on both of the cylinders increase, the (d)D_C_L^{RMS} is relatively stable and the (D)d_C_L^{RMS} increases at d/D=0.375, meanwhile, the amplitude of lift coefficient and drag coefficient on both of the cylinders increase also.

In Regime 2, all of the amplitude of lift coefficient and drag coefficient, (d)D_C_L^{RMS}, (D)d_C_L^{RMS} on both of the cylinders decreases rapidly, especially, the amplitude of drag coefficient nearly converge to zero from d/D=0.5 to d/D=0.875.

In Regime 3, the amplitude of lift coefficient and drag coefficient on both of the cylinders increase once more, (d)D_C_L^{RMS} continuous decrease and (D)d_C_L^{RMS} become increase again. (d)D_C_D^{MEAN} decreases and (D)d_C_D^{MEAN} increases in the whole range, both of these fluid coefficient are linear with diameter ratio, especially, (d)D_C_D^{MEAN} becomes a negative value from d/D=0.875 to d/D=1, it means that the direction of (d)D_C_D^{MEAN} becomes opposite to the streamwise.

ACKNOWLEDGEMENT

REFERENCES

Assi, G.R.S., Meneghini, J.R., Aranha, J.A.P., Bearman, P.W., Casaprima, E.(2006). "Experimental investigation of flow-induced vibration interference between two circular cylinders." Journal of Fluids and Structures 22, 819–827.

Bearman, P.W. (1967) "The effect of base bleed on the flow behind a two-dimensional model with a blunt trailing edge." The Aeronautical Quarterly 18, 207–224.

Bearman, P.W., Wadcock, A.J.(1973). "The interaction between a pair of circular cylinders normal to a stream." Journal of Fluid Mechanics 61, 499–511.

Khalak, A., Williamson, C.H.K., (1999). "Motion, forces and mode transitions in vortex-induced vibrations at low mass damping." Journal of Fluids and Structures 13, 813–851.

King, R., Johns, D.J. (1976) "Wake interaction experiments with two flexible circular cylinders in flowing water." Journal of Sound and Vibration 45, 259–283.

Laneville, A., Brika, D. (1999) "The fluid and mechanical coupling between two circular cylinders in tandem arrangement." Journal of Fluids and Structures 13, 967–986.

Laneville, A., Brika, D.(1999) "The fluid and mechanical coupling between two circular cylinders in tandem arrangement." Journal of Fluids and Structures 13, 967–986.

Mahir, N., Rockwell, D.(1996) "Vortex formation from a forced system of two cylinders, part 1: tandem arrangement." Journal of Fluids and Structures 10, 473–489.

Meneghini, J.R., Saltara, F., Siqueira, C.L.R., Ferrari Jr., J.A., (2001). "Numerical simulation of flow interference between two circular cylinders in tandem and side-by-side arrangements." Journal of Fluids and Structures 15, 327–350.

Mittal, S., Kumar, V., Raghuvanshi, A., (1997). "Unsteady incompressible flows past two cylinders in tandem and staggered arrangements." International Journal for Numerical Methods in Fluids 25, 1315–1344.

Williamson, C.H.K., Govardhan, R. (2004) "Vortex induced vibration." Annual Review of Fluid Mechanics 36, 413–455.

Williamson, C.H.K., Roshko, A.(1988). "Vortex formation in the wake of an oscillating cylinder." Journal of Fluids and Structures 2, 355–381.